Facile method to synthesize of magnesium-graphene nano sheets for candidate of primary battery electrode

by Rikson Asman Fertiles Siburian

Submission date: 13-Apr-2023 12:39PM (UTC+0700)
Submission ID: 2063242034
File name: 1-s2.0-S2215038222000292-main.pdf (10.14M)
Word count: 5243
Character count: 26001

Colloid and Interface Science Communications 48 (2022) 100612

Contents lists available at ScienceDirect

Colloid and Interface Science Communications

journal homepage: www.elsevier.com/locate/colcom

Rapid Communication

Facile method to synthesize of magnesium-graphene nano sheets for candidate of primary battery electrode

Rikson Siburian [a,b,*], Suriati Paiman [c], Fajar Hutagalung [a], Ab Malik Marwan Ali [d], Lisnawaty Simatupang [e], Ronn Goei [f], Mohamad Mahmood Rusop [g,h]

[a] Postgraduate Program, Chemistry Department, Faculty of Mathematics and Natural Sciences, Universitas Sumatera Utara, Medan 20155, Indonesia
[b] Carbon Research Center-Universitas Sumatera Utara, Medan, Indonesia
[c] Physics Department, Faculty of Science, Universiti Putra Malaysia, 43400 (Serdang) Seri Kembangan, Selangor, Malaysia
[d] Faculty of Applied Sciences, Universiti Teknologi MARA, 40450 Shah Alam, Selangor, Malaysia
[e] Department of Chemistry, Faculty of Mathematics and Natural Sciences, Universitas Negeri Medan, Jl. Willem Iskandar Psr. V, Medan, North Sumatera, 20221, Indonesia
[f] School of Materials Science and Engineering, Nanyang Technological University, 50 Nanyang Avenue, 639798, Singapore
[g] School of Electrical Engineering, College of Engineering, Universiti Teknologi MARA, 40450 Shah Alam, Selangor, Malaysia
[h] NANO-SciTech Lab (NST), Center for Functional Materials and Nanotechnology, Institute of Science (IOS), Universiti Teknologi MARA, 40450 Shah Alam, Selangor, Malaysia

ARTICLE INFO

Keywords:
Anode primary battery
Electrical conductivity
Graphene nano sheets
Mg/GNS
Primary battery electrode

ABSTRACT

The effect of particle sizes of Mg on Magnesium-Graphene nano sheets (Mg-GNS (C-π)) interaction when used as an anode of primary battery was evaluated. GNS was synthesized using the modified Hummers method, while Mg/GNS composite with 10–40% Mg was prepared by a facile impregnation method. XRD data of Mg/GNS shows peaks of C(002) and Mg(102) at $2\theta = 26.77^{\circ}$ and 44.69°, respectively, indicating Mg metals were successfully introduced onto GNS surfaces. These data are consistent with the EDX spectrum which shows peaks of C (0.277 keV) and Mg (1.253 keV). Mg 10%/GNS (3.871 μm) and Mg 30%/GNS (4.485 μm) have the smallest and largest metal particle size deposited, respectively. Mg 10%/GNS (62.9 μS/cm^2) has a higher electrical conductivity value than the bare GNS (61.4 μS/cm^2) and commercial primary battery anode (Zn plate, 35 μS/cm^2). The results obtained show that GNS is able to modify the metallic character of Mg (*p-s* interaction). Furthermore, the presence of Mg metal deposition on the GNS surface is able to produce Mg/GNS with increased electrical conductivity so that it could be used as an alternative anode primary battery.

1. Introduction

The primary battery is a convenient source of power for portable electric and electronic devices. Batteries carry chemical potential energy that can be easily converted to electrical energy through the reduction and oxidation processes happening at the anode and cathode. In a battery, electrons flow from the anode to the cathode. Then electrons from the cathode through the electrolyte are expected to flow to the anode (battery cycle). This process can occur when the battery is arranged in a closed circuit [1,2]. Some of the main problems found in the use and development of anode materials in commercial battery systems today are i) the dendritic growth at the surface of Li and graphite composite (LiC_6) anode when shows operated at high current densities and discharge rates causing internal short circuits and impairment of battery performance [3,4]; ii) shorter battery life due the limitation of Zn and Li metals in controlling the rate of electron mobility [5–7]; iii) the limited natural availability of Zn and Li due to higher production commercialization of primary battery [8],; and iv) poor energy density, electrical conductivity and capacity of the battery [9,10].

Graphene is a two-dimensional layer of carbon atoms arranged in a honeycomb lattice, demonstrates a variety of unique electronic and transport properties. The discovery of such fascinating phenomena such as a very high electron and hole mobilities, ambipolar electric field effect, integer and half-interger quantum Hall effects for electrons and holes, etc [11,12] has attracted a lot of attention from the different fields ranging from solid state physics and chemistry. The graphene

* Corresponding author at: Postgraduate Program, Chemistry Department, Faculty of Mathematics and Natural Sciences and Carbon Research Center, Universitas Sumatera Utara, Medan 20155, Indonesia.
E-mail address: rikson@usu.ac.id (R. Siburian).

https://doi.org/10.1016/j.colcom.2022.100612
Received 26 November 2021; Received in revised form 6 March 2022; Accepted 7 March 2022
Available online 12 March 2022

honeycomb lattice is composed of two equivalent sub-lattices of carbon atoms bonded together with σ bonds. Each carbon atom in the lattice has a π orbital that contributes to a delocalized network of electrons [13]. Graphene has a large theoretical specific surface area 2630 m^2g^{-1}, high intrinsic mobility 200,000 $cm^2v^{-1}s^{-1}$ high Young's modulus (~1.0 TPa) [14,15] as well as high thermal conductivity ~5000 $Wm^{-1}K^{-1}$, high optical transmittance (~97.7%) [16] and good electrical conductivity warrant an investigation for applications such as for transparent conductive electrodes [17,18], among many other potential applications. However, graphene has a valence band (π) and conduction band (π*) which overlap each other at the corner of the hexagonal Brillouine zone (K point) forming a Dirac point so that graphene has no energy band gap and is difficult to apply directly as a semiconductor material [19,20]. In addition, pure graphene still has a lower electrical conductivity compared to graphene alloys with metal [21]. Therefore, graphene needs to be modified in order to improve its electrical properties and electrical conductivity. The interaction between metal particles and graphene through the metal adsorption process by the graphene surface can improve and modify the electronic and magnetic properties of the bare graphene materials [22]. Graphene nano sheets (GNS) could reduce the occurrence of metal particle agglomeration, and thus are able to control the size distribution and distribution of metal particles deposited on the surface of the sheet [23–25]. The application of Mg/graphene alloys in the manufacture of battery electrodes was able to produce batteries with high performance (electrical conductivity, energy density and capacity) [21,26–29]. However, the effect of the interaction of GNS with Mg (a ns-block metal) and the concentration of Mg on the particle size of the metal deposited on the graphene surface and the performance (electrical conductivity) of the Mg/graphene alloy has not been fully understood. Therefore, this research needs to be done as a solution to these problems.

2. Experimental section

2.1. Materials

Graphite commercial powder, sulfuric acid (H_2SO_4, 98 wt%), potassium permanganate ($KMnO_4$, 99.5 wt%), hydrogen peroxide (H_2O_2, 30 wt%), and ammonia (NH_3, 25 wt%) were purchased from Sigma-Aldrich (Singapore). Sodium nitrate ($NaNO_3$, 99 wt%) and Magnesium chloride ($MgCl_2.6H_2O$, 99 wt%) were purchased from Merck (Singapore). All the chemical reagents were used without any further purification.

2.2. Preparation of GNS

First of all, 2 g of commercial graphite powder was put into an Erlenmeyer flask, then 2 g of $NaNO_3$ and 150 mL of 96% H_2SO_4 were added sequentially. The mixture was stirred for 2 h to produce a uniform solution. Next, 10 g of $KMnO_4$ was added to the solution slowly and stirred for 4 h in an ice bath. After 4 h, the Erlenmeyer flask was removed from the ice bath and stirred again for 72 h. After that, 200 mL of 5% H_2SO_4 was added to the solution, then stirred again for 2.5 h.

At the end of the 2.5 h, 10 mL of 30% H_2O_2 was added to the solution followed by a continued stirring for an additional 10 h. Next, the graphite oxide mixture was centrifuged using a centrifuge at a speed of 6500 rpm for 20 min to separate the supernatant and precipitate. The precipitate obtained was washed sequentially with piranha solution and distilled water until a clear supernatant (pH ~ 5–6) was obtained and then centrifuged again for 20 min at 6500 rpm. The final precipitate was suspended in 100 mL distilled water to obtain a uniform GO solution through 5 h ultrasonication treatment.

Next, 10 mL of 10 M NH_3 were added to 100 mL of graphene oxide solution and stirred for 72 h to produce a mixture. Next, the mixture was filtered through Whatmann No. 42 filter paper. The graphene precipitate obtained was dried in an oven at 100 °C for 2 h.

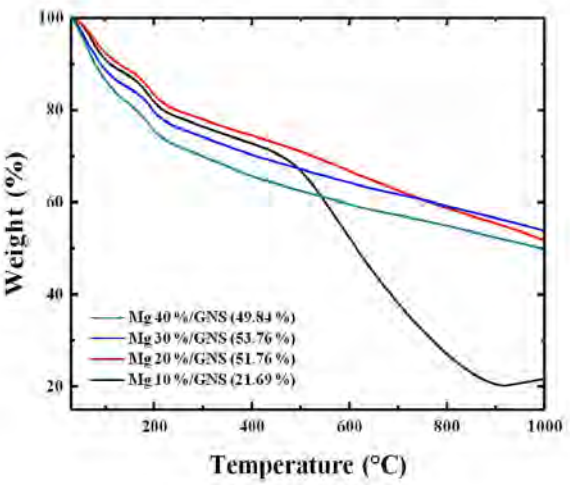

Fig. 1. TGA data of Mg/GNS.

2.3. Preparation of Mg 10, 20, 30, 40%/GNS

A total of 0.5 g of GNS powder and 0.4647 g of $MgCl_2.6H_2O$ crystals were added to each of 20 mL of ethanol and stirred for 1 h to produce a mixture of GNS and Mg precursor solution. Next, GNS solution and Mg precursor solution were mixed and stirred for 3 h to produce a Magnesium-GNS mixture. The Magnesium-GNS mixture was filtered through Whatmann No. 42 filter paper to separate the filtrate and precipitate. The precipitate obtained was dried at 80 °C for 2 h, producing a solid powder and labeled as Mg 10%/GNS. The same procedure was carried out to prepare Mg 20, 30, and 40%/GNS with the amount of crystalline of $MgCl_2.6H_2O$ mass added were 1.0456 g, 1.7924 g, and 2.7882 g, respectively [30,31].

3. Results and discussion

3.1. Thermogravimetric analysis (TGA)

TGA was conducted to determine the weight percentage of Mg metal deposited on the GNS surface. Weight percentage analysis of Mg metal in Mg/GNS was carried out using a TGA instrument type Netzsch TG 209F3 TGA in N_2 atmosphere with a temperature range of 30–1000° C (10.0 K/min). TGA data for Mg/GNS composites can be seen in Fig. 1.

The thermogram pattern of Mg/GNS shows that Mg 10%/GNS has a different thermogram pattern as compared with Mg 20, 30 and 40%/GNS. This is because of the size of the Mg particles deposited on the GNS surface is not the same. The Mg/GNS thermogram pattern shows that the character of Mg particles deposited on the surface of GNS is not linear with respect to the mass of Mg precursors. This means that the character of Mg metal can be modified by the interaction between deposited Mg with the GNS substrate. Mg 10%/GNS has a relatively higher weight loss of graphene starting at 500° C compared to Mg 20, 30 and 40%/GNS. This is due to Mg 10%/GNS has the smallest size and number of Mg particles deposited on the graphene surface (as confirmed by observation through Scanning Electron Microscope (SEM)).

3.2. X-Ray diffraction (XRD)

Analysis of Mg/GNS material with XRD was carried out to prove that Mg metal had been deposited, as well as to determine the size of Mg particles deposited on the surface of GNS. Structural analysis of Mg 10–40%/GNS was performed using a panAlytical X-ray diffractometer instrument with a Cu–Kα radiation detector (1.54051 Å) in a scan range

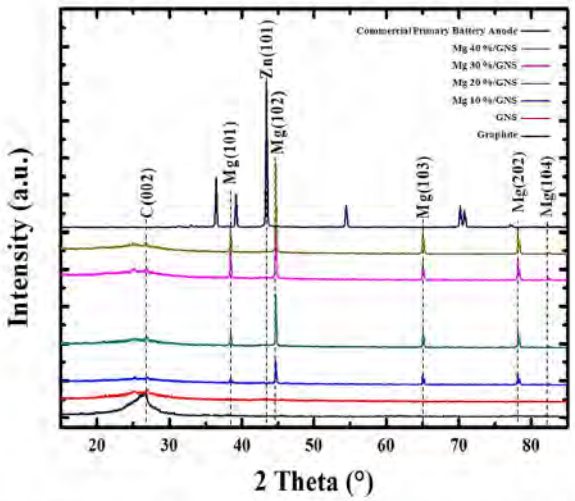

Fig. 2. Diffractogram of commercial primary battery anode, graphite, GNS, and Mg/GNS.

of

2°–90°, scan speed of 5° min^{-1}, voltage of 45 kV and a current of 40 mA. The diffractogram of graphite, GNS, commercial primary battery anode (Zn plate) and Mg/GNS are shown in Fig. 2.

XRD pattern of graphite and GNS showed peaks of C(002) at positions 2θ = 26.77° (d-spacing 3.327 nm) and 2θ = 26.85° (d-spacing 3.317 nm) (JCPDS 75–2078). While the anode of commercial primary battery shows a peak at position 2θ = 43° which indicates that the anode of commercial primary battery is consists predominantly of Zn metal. The diffractogram pattern of Mg/GNS shows the presence of weak and wide peaks at positions.

2θ = 26.77° (3.327 Å) (JCPDS 75–2078; C(002) GNS: 26.55° (3.354 Å)). In addition, the diffraction peaks of Mg(102) which appear at 2θ = 44.69° (JCPDS 78–0430: Mg(102) 44.69° (2.026 Å)) [27,28] proved that Mg metal particles are successfully deposited on the GNS surface.

Mg particles deposited on the surface of the GNS form clusters. There are two main factors that influence the formation of Mg clusters on the GNS surface, namely the entropy factor and the enthalpy factor. For the entropy factor, its known that GNS has a large surface area as a supporting material and is able to modify the electron states of metal particles [30–33]. The second factor (enthalpy factor), caused by the overlapping of C–$p_{x/y}$ orbitals (graphene) with Mg–2 *s* (strong *p-s* hybridization) which causes electron transfer from graphene to Mg (p-doping graphene). Interfacial hybridization between Mg-graphene can open up the graphene energy gap (ΔEK = 0.42 eV) [22,34,35] and hence, is able to change the character of Mg metal and modify the particle size of Mg metal deposited on the graphene surface [19,22,36].

3.3. SEM-EDX

Analysis of surface morphology and elemental abundance in commercial primary battery anode, graphite, GNS, and Mg 10–40%/GNS was carried out using a Phenom type SEM instrument with a voltage of 5 kV, while a voltage of 15 kV was used for EDX mapping. The surface morphology and components of Mg 10–40%/GNS are shown in Figs. 3 and 4.

Fig. 3(a) shows the anode surface of a commercial primary battery in the form of lumps that accumulate like a pile of needles. Graphite SEM results (Fig. 3(b)) show that commercial graphite is composed of non-uniform piles with a dense, thick, and very dense structure which indicates that graphite has layered structure. Fig. 3(c) shows that GNS substrate consists of a smaller particle size with wrinkled surface and edges. These graphene sheets are arranged randomly and closely linked between layers to form irregular aggregates with layers that are thinner than graphite. The SEM image of Mg/GNS (Fig. 3(d-g)) shows that in each image there are small white spots (indicated by objects in blue circles) which are clustered Mg particles attached to thin sheets (GNS, indicated by brown arrows). The results of SEM and EDX mapping of

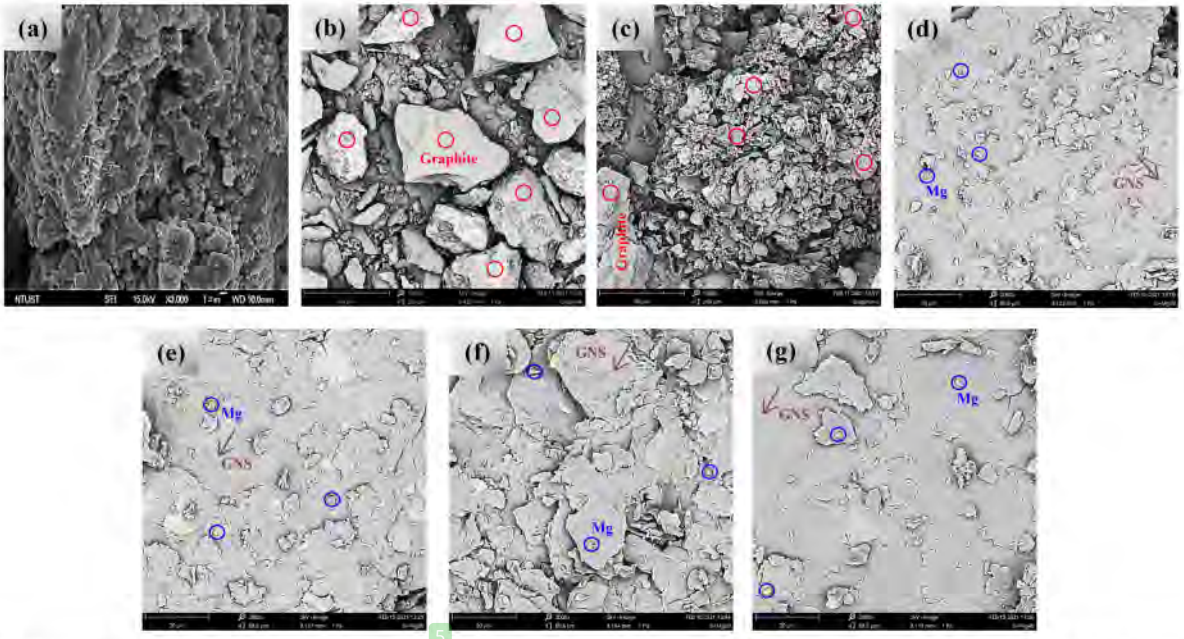

Fig. 3. SEM images of commercial primary battery anode (a), graphite (b), GNS (c), Mg 10%/GNS (d), Mg 20%/GNS (e), Mg 30%/GNS (f) and Mg 40%/GNS (g).

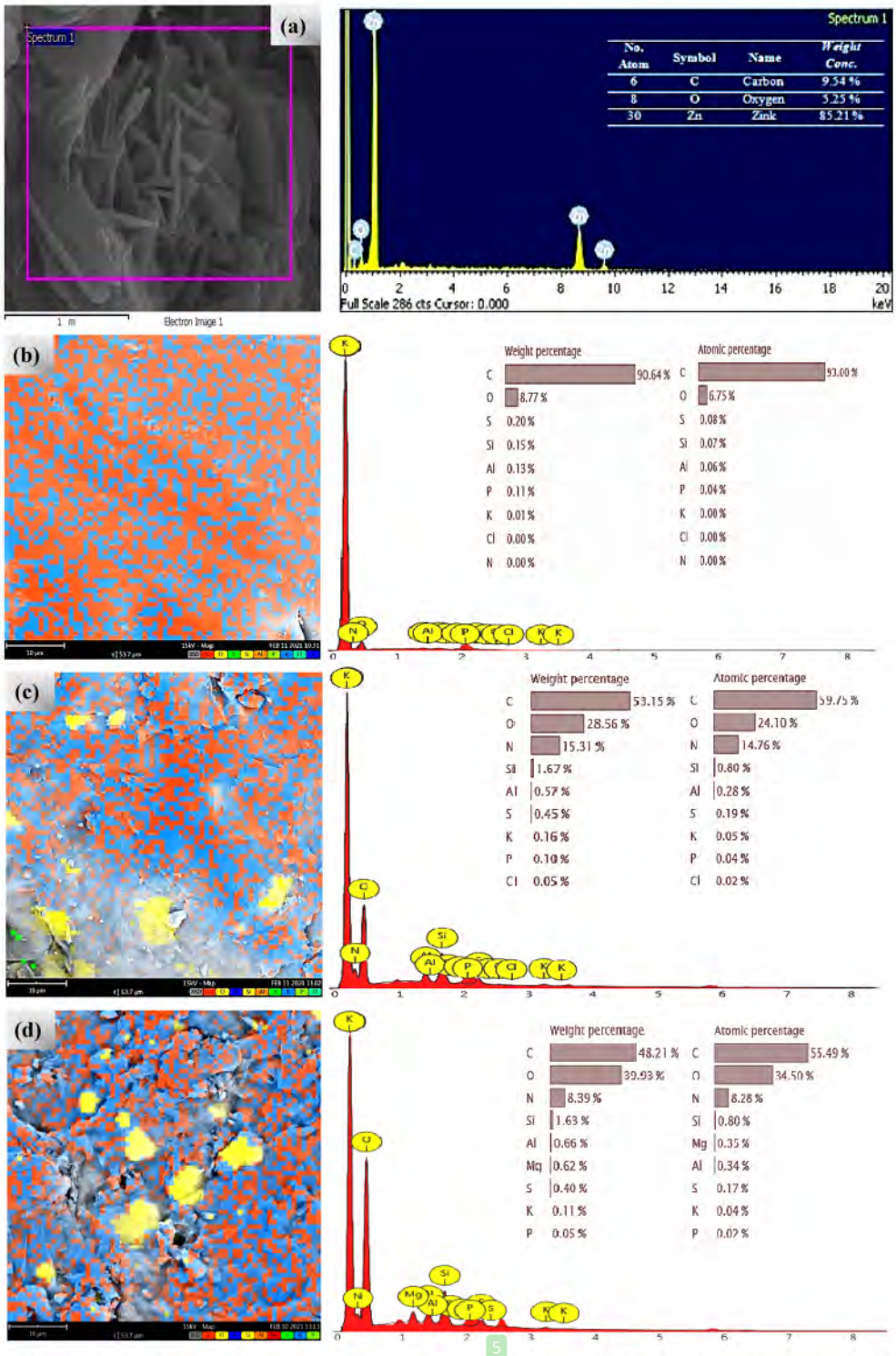

Fig. 4. Mapping SEM images and EDX Spectrum of commercial primary battery anode (a), graphite (b), GNS (c), Mg 10%/GNS (d), Mg 20%/GNS (e), Mg 30%/GNS (f) and Mg 40%/GNS (g).

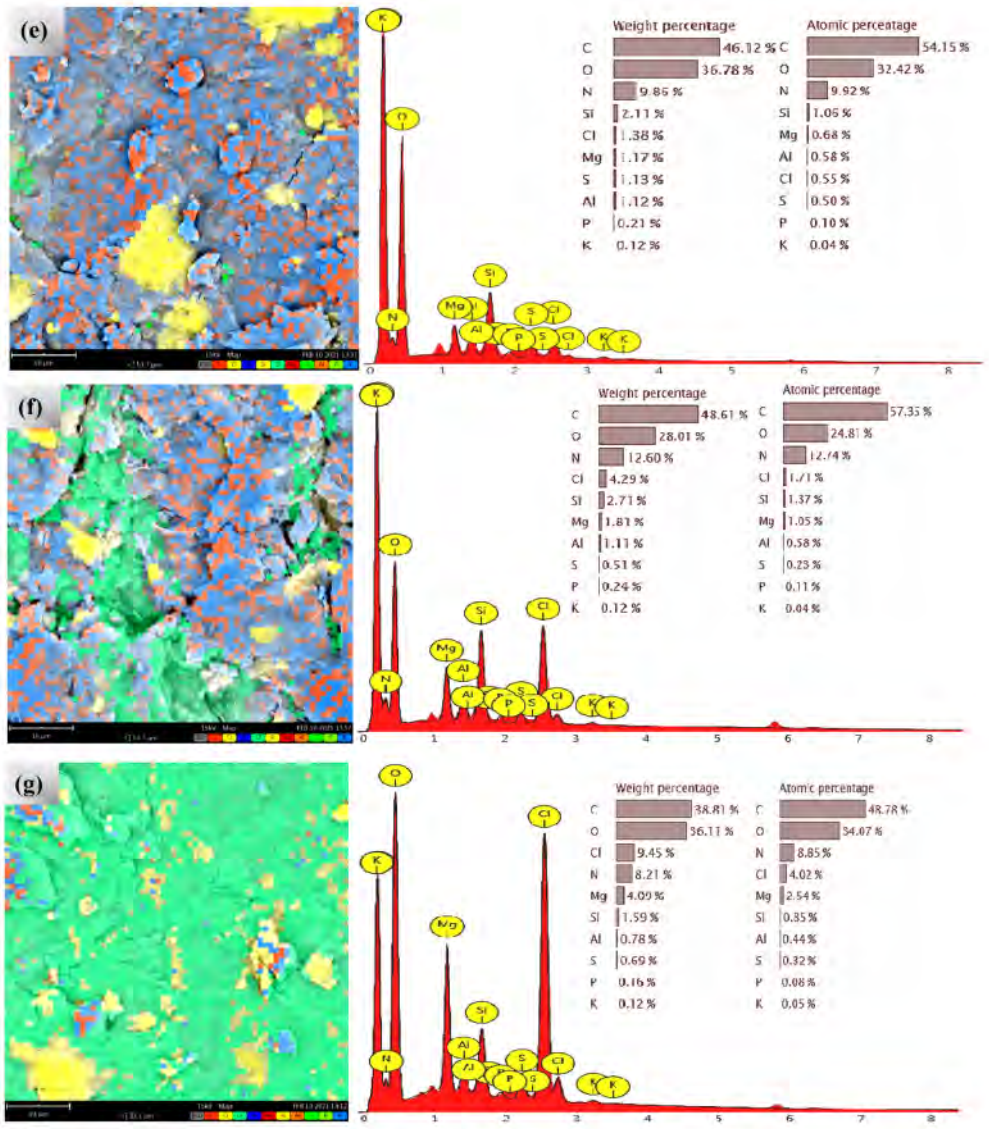

Fig. 4. (*continued*).

graphite (Fig. 4 (b)) shows that the abundance of constituent elements graphite is dominated by C atoms (~90.64%). The presence of other elements in graphite as detected by EDX such as O, S, Si, Al, P and K with a small mass concentration indicates that the commercial graphite used is not pure. When compared with the results of EDX graphite, it can be observed that in the GNS structure there is a decrease in the concentration of element C (to 59.8%) and is accompanied by an increase in the concentration of several elements such as O, N, and K (Fig. 4 (c)). This is due to the use of strong oxidizing agents (H_2SO_4, $KMNO_4$, and H_2O_2) during the graphite oxidation process and NH_3 reducing agents during the reduction of graphene oxide to graphene.

The mapping of Mg/GNS shows the abundance of Mg/GNS constituent elements, where in each material there is the presence of Carbon (GNS) and Mg elements. This indicates that the Mg metal particles have been deposited and spread evenly on the surface of the GNS. Furthermore, EDX analysis was used to qualitatively prove the presence of Mg deposited on the GNS surface. The EDX spectrum of Mg/GNS showed peaks at the energy values of 0.277 keV and 7.472 keV for Carbon (C) and Magnesium (Mg), respectively. The weight and atomic percentages of Mg deposited in the GNS increased in number with the increase in weight % of the Mg precursors. These results prove that each of the Mg metal has been deposited on the surface of the GNS. The EDX spectrum of Mg/GNS also showed the presence of other elements (Al and Si) which were not derived from the chemicals used in the study. These were caused by the material residue left on the sample holder. Fig. 5 also shows the size distribution and average size of Mg particles in Mg/GNS. The size of the deposited Mg particles is not linear with the concentration of Ni metal. Mg 10%/GNS has the smallest average Mg particle size of 3.871 μm and Mg 30%/GNS has the largest average Mg particle size of 4.485 μm. Mg/GNS has a homogeneous deposited metal particle size distribution on the GNS surface. This proves that GNS is able to modify the character of Mg particles.

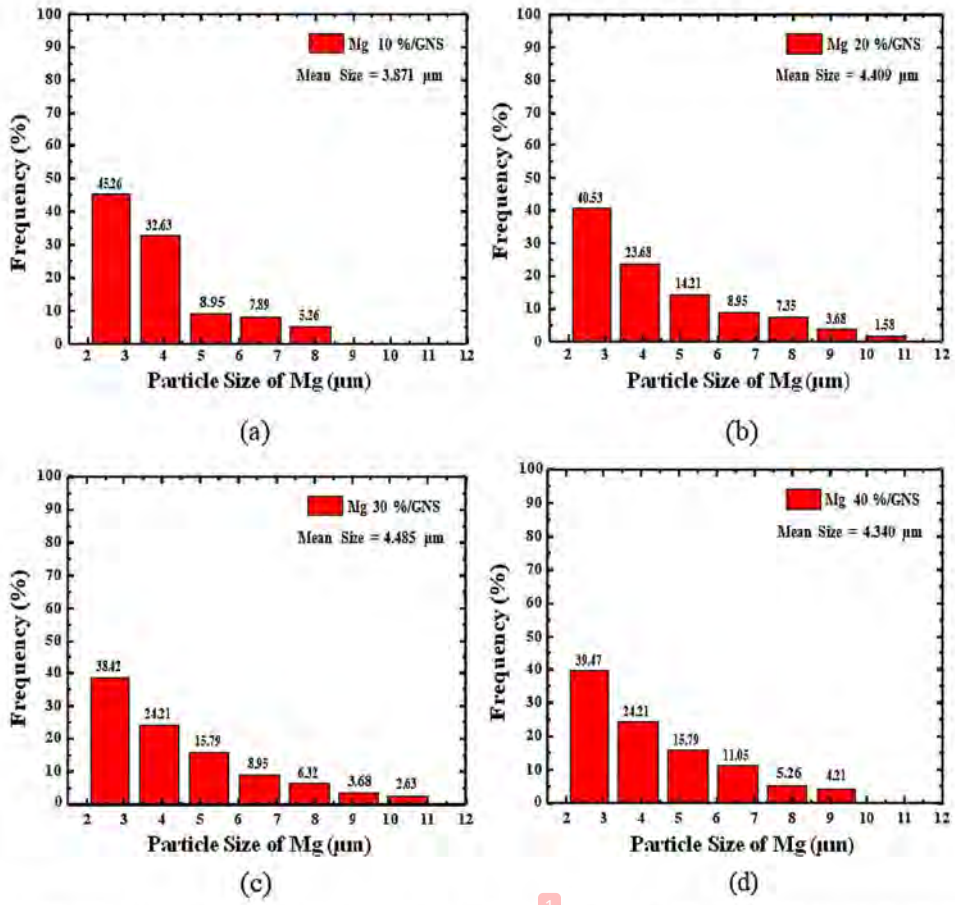

Fig. 5. Average size of Mg particles deposited on GNS surface: Mg 10%/GNS (a); Mg 20%/GNS (b); Mg 30%/GNS (c); and Mg 40%/GNS (d).

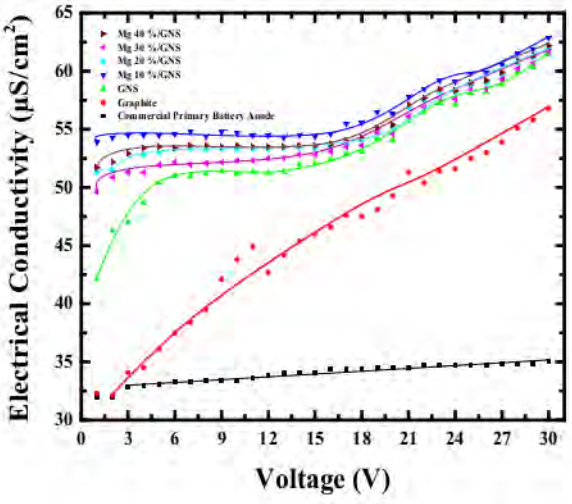

Fig. 6. Electrical Conductivity of Commercial Primary Battery Anode (Zn plate), Graphite, GNS and Mg/GNS at a voltage of 1–30 V.

3.4. Electrical conductivity analysis

Electrical conductivity analysis was carried out to determine the effect of the size of the Mg metal deposited on the surface of the GNS on the activity of Mg/GNS in conducting electric current. Electrical conductivity analysis was carried out on each sample using a fuse tube (length = 2.3 cm; diameter = 0.3 cm) containing each sample (mass = 0.15 g) combined with a DC Power Supply instrument CODY 3005DT and a ZOTEK ZT98 digital multimeter.

The measurement of the electrical conductivity of the battery anode is carried out at a voltage of 1–30 V. This aims to determine the stability and strength of the electron mobility of each material in conducting electrical current to the maximum achievable voltage (30 V). The results of the electrical conductivity measurements of Commercial Primary Battery Anode (Zn plate), graphite, GNS and Mg/GNS at a voltage of 1–30 V are shown in Fig. 6.

Fig. 6 shows that the electrical conductivity of a commercial primary battery anode (Zn plate) shows a constant increasing value. This proves that the anode of the primary battery is good enough to control the rate of electron mobility. GNS has a higher electrical conductivity value than commercial primary battery anodes. This is because GNS has delocalized electrons along the C = C bond which would acts as an electric charge carrier. In addition, GNS also has a large surface area that would increase the rate of electron mobility [37]. The value of electrical conductivity in the GNS increased significantly at a voltage of 1–9 V, then

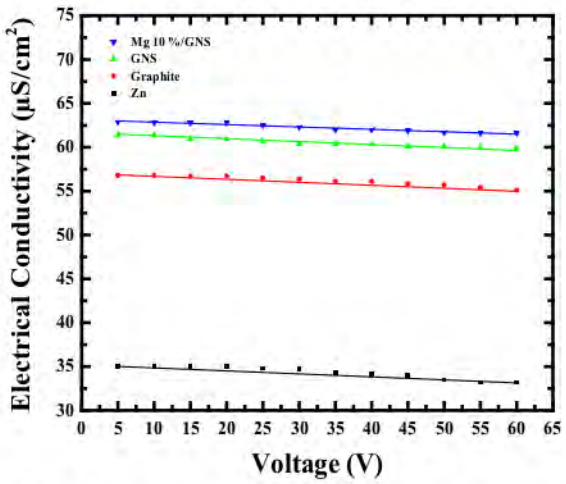

Fig. 7. Relationship of Electrical Conductivity (μS/cm^2) with Time (minutes) of commercial primary battery anode (Zn plate), Graphite, GNS, and Mg 10%/GNS.

decreased at a voltage of 10–14 V, and increased again at a voltage of 14–30 V. This proves that the GNS is still difficult to control the mobility of electrons flowing through the external circuit. Mg/GNS has an increased electrical conductivity value and tends to be more stable than GNS. The result presented is in agreement with previously published datat that suggested that the increase the stability of the flow rate of electron mobility of metal-graphene composite was caused by a high surface to volume ratio of the composite [38]. The electrical conductivity of Mg/GNS increases constantly at a voltage of 1–6 V. Under these conditions, the electron flow rate increases gradually as the voltage increases. Electron mobility becomes more stable at voltage 6–21 V. In this condition, the electron flow rate is laminar (laminar flow), where the kinetic energy of the electrons increases constantly, so the electrical conductivity increases slowly (more stable). At a higher voltages (21–30 V), the kinetic energy of electrons used to move from the valence band to the conduction band increases excessively (turbulence flow) so that the electron flow rate becomes more active and faster so as to reduce the resistivity and increase the electrical conductivity value of the electron significantly in each material. This proves that the greater the electric voltage applied to a material can increase the number and rate of electron mobility that flows.

Mg 10%/GNS (62.9 μS/cm^2) has the highest electrical conductivity value at the maximum voltage (30 V). This is because Mg 10%/GNS has the smallest average size of Mg metal particles deposited among other Mg/GNS (confirmed by SEM data). The electrical conductivity values of Mg/GNS are each influenced by the size of the Mg metal particles deposited on the surface of the GNS. This is because the smaller the size of metal particles deposited on the surface of the GNS would increase the surface contact area with the GNS so that it can increase the activity of the GNS in conducting electric current (increased electrical conductivity). The use of metal clusters on graphene with smaller sizes can produce materials with a more stable reactivity and electrical properties as well as a higher electrical conductivity values [38]. Furthermore, to find out the comparison of the stability of commercial primary battery anodes (Zn plates), graphite, GNS, and Mg 10%/GNS in conducting electric current, electrical conductivity measurements were carried out for each material at a constant voltage (30 V) with a time variation of 5–60 min. Electrical conductivity measurements were carried out at a voltage of 30 V because at the given voltage value, the maximum electrical conductivity value of each material was obtained. The electrical conductivity values of each material obtained at a voltage of 30 V (5–60 min) are shown in Fig. 7.

Fig. 7 shows that the Zn plate (commercial primary battery anode) has the largest reduction in electrical conductivity value (5.14%) compared to GNS (2.44%), and Mg 10%/GNS (2.07%) at 5–60 min and a constant voltage of 30 V. This is influenced by the nature of Zn metal which easily loses electrons at a given high voltage (30 V).

4. Conclusions

The interaction between GNS (supporting material) and Mg metal (*p-s*) can modify the character of Mg metal (ionic). The size of the Mg particles deposited on the GNS surface is not linear with the Mg precursor concentration. Mg 10%/GNS each has the smallest average size of Mg metal particles deposited in GNS, which is 3.871 μm, while Mg 30%/GNS has the largest average size of Mg metal particles deposited in GNS, which is 4.485 μm (SEM data). Mg 10%/GNS (62.9 μS/cm^2) has a higher electrical conductivity value than graphite GNS (61.4 μS/cm^2) and commercial primary battery anode (Zn plate, 35 μS/cm^2) suggesting the potential of Mg-GNS to be used as an alternative primary battery anode.

Declaration of Competing Interest

The authors declare no competing financial interest.

Acknowledgments

We would like to thankful to Direktur Sumber Daya, Direktorat Jenderal Pendidikan Tinggi, Riset dan Teknologi and LPDP who Funding Support this research under World Class Professor (WCP) Skim Program Nomor 2817/E4.1/KK.04.05/2021.

References

[1] Y. Dong, J. Li, F. Yang, Y. Wang, Z. Zhang, J. Wang, Y. Long, X. Wang, Bioresorbable primary battery anodes built on Core–double-Shell zinc microparticle networks, ACS Appl. Mater. Interfaces 13 (2021) 14275–14282.
[2] Y. Li, Y. Lu, P. Adelhelm, M.M. Titirici, Y.S. Hu, Intercalation chemistry of graphite: alkali metal ions and beyond, Chem. Soc. Rev. 48 (2019) 4655–4687.
[3] A. Jana, D.R. Ely, R.E. García, Dendrite-separator interactions in lithium-based batteries, J. Power Sources 275 (2015) 912–921.
[4] M.R. Al Hassan, A. Sen, T. Zaman, M.S. Mostari, Emergence of graphene as a promising anode material for rechargeable batteries: a review, Mater. Today Chem. 11 (2019) 225–243.
[5] C. Hou, Q. Zhang, M. Zhu, Y. Li, H. Wang, One-step synthesis of magnetically-functionalized reduced graphite sheets and their use in hydrogels, Carbon 49 (2011) 47–53.
[6] Q. Wang, C. Zhang, H. Jung, P. Liu, D. Patel, S.G. Pavlostathis, Y. Tang, Transformation and mobility of Cu, Zn, and Cr in sewage sludge during anaerobic digestion with pre- or interstage hydrothermal treatment, Environ. Sci. Technol. 55 (2021) 1615–1625.
[7] Q. Guo, W. Zeng, S.-L. Liu, Y.Q. Li, J.-Y. Xu, J.-X. Wang, Y. Wang, Recent developments on anode materials for magnesium-ion batteries: a review, Rare Metals 40 (2020) 290–308.
[8] J.F. Parker, C.N. Chervin, I.R. Pala, M. Machler, M.F. Burz, J.W. Long, D.R. Rolison, Rechargeable nickel-3D zinc batteries: an energy-dense, safer alternative to lithium-ion, Science 356 (2017) 415–418.
[9] B. Yan, M.S. Li, X.F. Li, Z.M. Bai, J.W. Yang, D.B. Xiong, D.J. Li, Novel understanding of carbothermal reduction enhancing electronic and ionic of $Li_4Ti_5O_{12}$, J. Mater. Chem. A 3 (2015) 11773–11781.
[10] X. Wang, Q. Weng, Y. Yang, Y. Bando, D. Golberg, Hybrid two-dimensional materials in rechargeable battery applications and their microscopic mechanisms, Chem. Soc. Rev. 45 (2016) 4042–4073.
[11] K.S. Novoselov, A.K. Geim, S.V. Morozov, D. Jiang, M.I. Katsnelson, I. V. Grigorieva, S.V. Dubonos, A.A. Firsov, Two-dimensional gas of massless Dirac fermions in graphene, Nature 438 (2005) 197–200.
[12] Y. Zhang, Y. Tan, H.L. Stormer, P. Kim, Experimental observation of the quantum Hall effect and Berry's phase in graphene, Nature 438 (2005) 201–204.
[13] Z. Yanwu, M. Shanthi, C. Weiwei, L. Xuesong, W.S. Ji, R.P. Jeffrey, S.R. Rodney, Graphene and graphene oxide: synthesis, properties, and application, Adv. Mater. 22 (2011) 3906.
[14] K.I. Bolotin, K.J. Sikes, Z. Jiang, M. Klima, G. Fudenberg, J. Hone, P. Kim, H. L. Stormer, Ultrahigh electron mobility in suspended graphene, Solid State Commun. 146 (2008) 351–355.
[15] S.V. Morozov, K.S. Novoselov, M.I. Katsnelson, F. Schedin, D.C. Elias, J. A. Jaszczak, A.K. Geim, Giant intrinsic carrier Mobilities in graphene and its bilayer, Phys. Rev. Lett. 100 (2008), 016602.

[16] A.A. Balandin, S. Ghosh, W.Z. Bao, I. Calizo, D. Teweldebrhan, F. Miao, C.N. Lau, Superior thermal conductivity of single-layer graphene, Nano Lett. 8 (2008) 902–907.
[17] W. Cai, Y. Zhu, X. Li, R.D. Piner, R.S. Ruoff, Large area few-layer graphene/graphite films as transparent thin conducting electrodes, Appl. Phys. Lett. 95 (2009), 123115.
[18] X. Li, Y. Zhu, W. Cai, M. Borysiak, B. Han, D. Chen, R.D. Piner, L. Colombo, R. S. Ruoff, Transfer of large-area graphene films for high-performance transparent conductive electrodes, Nano Lett. 9 (2009) 4359.
[19] Y. Dedkov, E. Voloshina, Graphene growth and properties on metal substrates, J. Phys. Condens. Matter 27 (2015) 1–28.
[20] D. Ratih, R. Siburian, Andriayani., The performance of graphite/N-graphene and graphene/N-graphene as electrode in primary cell batteries, Rasayan J. Chem. 11 (2018) 1649–1656.
[21] C. Simanjuntak, R. Siburian, H. Marpaung, Tamrin., Properties of Mg/graphite and mg/graphene as cathode electrode on primary cell battery, Heliyon 6 (2020), e03118.
[22] X. Liu, C.Z. Wang, M. Hupalo, H.Q. Lin, K.M. Ho, M.C. Tringides, Metals on graphene: interactions, growth morphology, and thermal stability, Crystals 3 (2013) 79–111.
[23] Z.S. Wu, G. Zhou, L.C. Yin, W. Ren, F. Li, H.M. Cheng, Graphene/metal oxide composite electrode materials for energy storage, Nano Energy 1 (2012) 107–131.
[24] Z. Li, X. Ge, C. Li, S. Dong, R. Tang, C. Wang, Z. Zhang, L. Yin, Rational microstructure design on metal–organic framework composites for better electrochemical performances: design principle, synthetic strategy, and promotion mechanism, Small Methods 4 (2020) 1900756.
[25] D. Nandi, V.B. Mohan, A.K. Bhowmick, D. Bhattacharyya, Metal/metal oxide decorated graphene synthesis and application as supercapacitor: a review, J. Mater. Sci. 55 (2020) 6375–6400.
[26] J.C. Pramudita, D. Pontiroli, G. Magnani, M. Gaboardi, C. Milanese, G. Bertoni, N. Sharma, M. Riccò, Effect of Ni-nanoparticles decoration on graphene to enable high capacity sodium-ion battery negative electrodes, Electrochim. Acta 250 (2017) 212–218.
[27] M. Rashad, F. Pan, A. Tang, M. Asif, J. She, J. Gou, J. Mao, H. Hu, Development of magnesium-graphene nanoplatelets composite, J. Compos. Mater. 49 (2015) 285–293.
[28] L. Malyala, S. Thatipamula, V.R. Jetti, Magnesium–graphene composite coated on SS mesh as cathode material for rechargeable magnesium ion battery, Trans. Indian Inst. Metals 72 (2019) 2503–2510.
[29] A. Mukanova, A. Zharbossyn, A. Nurpeissova, S.S. Kim, M. Myronov, Zh. Bakenov, Electrochemical study of graphene coated nickel foam as an anode for lithium-ion battery, Eurasian Chemico-Technol. J. 20 (2018) 91–97.
[30] R. Siburian, J. Nakamura, Formation process of Pt subnano-clusters on graphene Nanosheets, J. Phys. Chem. C 116 (2012) 22947–22953.
[31] R. Siburian, T. Kondo, J. Nakamura, Size control to a sub-nanometer scale in platinum catalysts on graphene, J. Phys. Chem. C 117 (2013) 3635–3645.
[32] T. Ohta, A. Bostwick, T. Seyller, K. Horn, E. Rotenberg, Controlling the electronic structure of bilayer graphene, Science 313 (2006) 951–954.
[33] K. Thakur, B. Kandasubramanian, Graphene and graphene oxide-based composites for removal of organic pollutants: a review, J. Chem. Eng. Data 64 (2019) 833–867.
[34] H. Tachikawa, T. Iyama, H. Kawabata, MD simulation of the interaction of magnesium with graphene, Thin Solid Films 518 (2009) 877–879.
[35] M. Tayyab, A. Hussain, Q. Asif, W. Adil, Band-gap tuning of graphene by mg doping and adsorption of Br and be on impurity: a DFT study, Comp. Condensed Matter E00469 (2020).
[36] A. Dahal, M. Batzill, Graphene-nickel interfaces: a review, Nanoscale 6 (2014) 2548–2562.
[37] S.M. Choi, M.H. Seo, H.J. Kim, W.B. Kim, Synthesis and characterization of graphene-supported metal nanoparticles by impregnation method with heat treatment in H_2 atmosphere, Synth. Met. 161 (2011) 2405–2411.
[38] F.M. Alvaro, J. Oliva, M. Herrera-Trejo, H.M. Hdz-García, A.I. Mtz-Enriquez, Icosahedral transition metal cluster (M_{13}, M = Fe, Ni, and cu) adsorbed on graphene quantum dots, Phys. E: Low-Dim. Syst. Nanostruct. 110 (2019) 52–58.

Facile method to synthesize of magnesium-graphene nano sheets for candidate of primary battery electrode

ORIGINALITY REPORT

14%	15%	11%	5%
SIMILARITY INDEX	INTERNET SOURCES	PUBLICATIONS	STUDENT PAPERS

PRIMARY SOURCES

1	123dok.com Internet Source	2%
2	carneylab.ucdavis.edu Internet Source	2%
3	C. Simanjuntak, R. Siburian, H. Marpaung, Tamrin. "Properties of Mg/graphite and Mg/graphene as cathode electrode on primary cell battery", Heliyon, 2020 Publication	2%
4	docksci.com Internet Source	2%
5	www.me.utexas.edu Internet Source	1%
6	www.researchsquare.com Internet Source	1%
7	riuma.uma.es Internet Source	1%
8	www.slideshare.net Internet Source	

		1 %
9	journals.utm.my Internet Source	1 %
10	ouci.dntb.gov.ua Internet Source	1 %
11	mafiadoc.com Internet Source	1 %
12	repository.usu.ac.id Internet Source	1 %
13	www.ccspublishing.org.cn Internet Source	1 %

Exclude quotes	Off	Exclude matches	< 1%
Exclude bibliography	On		